

**SURVEYING VESTA'S STYLES OF SPACE WEATHERING AND SURFACE MIXING.** D.T. Blewett<sup>1</sup>, B.W. Denevi<sup>1</sup>, T. Roatsch<sup>2</sup>, S.E. Schröder<sup>2</sup>, F. Tosi<sup>3</sup>, M.C. De Sanctis<sup>3</sup>, V. Reddy<sup>4</sup>, L. Le Corre<sup>4</sup>, C.M. Pieters<sup>5</sup>, C.A. Raymond<sup>5</sup>, and C.T. Russell<sup>6</sup>. <sup>1</sup>Johns Hopkins University Applied Physics Laboratory, Laurel, USA (david.blewett@jhuapl.edu); <sup>2</sup>Deutsches Zentrum für Luft- und Raumfahrt (DLR), Berlin, Germany; <sup>3</sup>Istituto di Astrofisica e Planetologia Spaziali, INAF, Rome, Italy; <sup>4</sup>Planetary Science Institute, Tucson, USA. <sup>5</sup>Brown University, Providence, USA; <sup>6</sup>JPL/Caltech, Pasadena, USA; <sup>7</sup>University of California, Los Angeles, USA.

**Introduction:** The *Dawn* spacecraft's mission at Vesta [1] has revealed a world that, although much smaller than the Moon or Mercury, has experienced planet-like processes and undergone a complicated geological evolution [2]. One fascinating characteristic of Vesta is the manner in which the regolith evolves in response to exposure to the space environment. In general, vestan space weathering is dominated by admixture of low-reflectance material delivered by carbonaceous chondrite (CC) impactors [3-7]. As a result, freshly exposed vestan basaltic material tends to become darker with time, and the strong absorption bands (near 1000 and 2000 nm) caused by ferrous iron in pyroxene become shallower. Darkening and decreased band contrast are hallmarks of lunar space weathering, however on the Moon these are accompanied by a strong increase in the continuum slope (reddening) [e.g., 8, 9]. The cause of the spectral changes on the Moon is the accumulation of micro- and nanophase metallic iron as a result of melting and vaporization by micrometeoroid bombardment and/or solar-wind sputtering [reviewed by 10].

We are conducting a survey of impact mixing and regolith maturation trends in different regions of Vesta. The goals are to document the range of space weathering styles on Vesta, and to examine how the observed trends can give clues to the composition of the material that is undergoing space weathering. The findings should help to further understanding of space weathering in the asteroid belt, and hence as a general phenomenon across the Solar System. Here we present results from two locations that illustrate Vesta's spectral diversity: Vibidia crater and near Oppia crater.

**Data:** Multispectral images from the *Dawn* Framing Cameras (FC) in seven narrow wavelength bands between 438 and 965 nm have been calibrated and photometrically normalized [11, 12], and mosaicked into quadrangle tiles [13] with a nominal pixel dimension of 60 m. The *Dawn* Visible and Infrared (VIR) imaging spectrometer [14-16] provides data to characterize the reflectance at high spectral resolution. We utilize two-dimensional (2D) histogram scatterplots of FC color ratios to examine spectral trends in selected image regions-of-interest (ROIs). The ratio of 917-nm reflectance divided by 749-nm reflectance (NIR ratio) is a measure of the depth of the 1000-nm Fe<sup>2+</sup> absorption, with lower ratio values corresponding to a strong-

er band. The 438-nm/749-nm ratio gauges the spectral slope at visible (Vis) wavelengths; a greater value of the ratio indicates a flatter ("bluer") slope.

**Vibidia crater:** Vibidia is an ~8-km diameter impact crater in the Tuccia (Av-13) quadrangle [17]. The crater has bright rays, and dark material is exposed on the floor and northern rim. An ROI extending from near the rim to the SW was defined (Fig. 1), covering both the bright continuous ejecta and the background surface. The 2D histograms (Figs. 1 and 2) illustrate the typical Vesta space-weathering changes [3]: The bright rays have stronger absorption bands, while the more mature background has lower reflectance and weaker bands, and has a flatter slope in the Vis, consistent with a greater abundance of CC-like material.

**Oppia "orange" patches:** The ejecta of Oppia crater (34-km diam.) has a very steep Vis slope, and has a distinctive appearance in the color-ratio presentations used by the *Dawn* team [18], largely because of a low 438-nm/749-nm ratio. Several related patches of this distinctive material are found to the NE of Oppia [18, 19]. These enigmatic features (Fig. 3) show strong color contrast with the surroundings, but no morphological differences are apparent even in the highest-resolution FC images (~20 m/pixel). A ROI was drawn to include the bright ejecta of a small (800-m) crater within one patch, a portion of the same patch, and some of the nearby normal background. The scatterplots (Figs. 3 and 4) reveal the striking difference in behavior between the NIR and the Vis. The NIR ratio scatterplot shows an orderly progression in band depth and reflectance, essentially linear two-endmember mixing. The Vis plot, on the other hand, exhibits more complicated structure, with a clear clustering of pixels in the unusual material that is separate from the background. One hypothesis is that the Vis spectral characteristics are caused by the presence of impact melt [19]. The spectral relationships suggest that the 800-m crater did not penetrate the patch and expose normal background material because the patch crater ejecta does not resemble fresh background material (spectrum #3 versus #4 in Figs. 3 and 4). We are in the process of making comparisons between VIR spectra and spectra of Fe-bearing silicate glasses [20, 21] to further understand the unusual material.

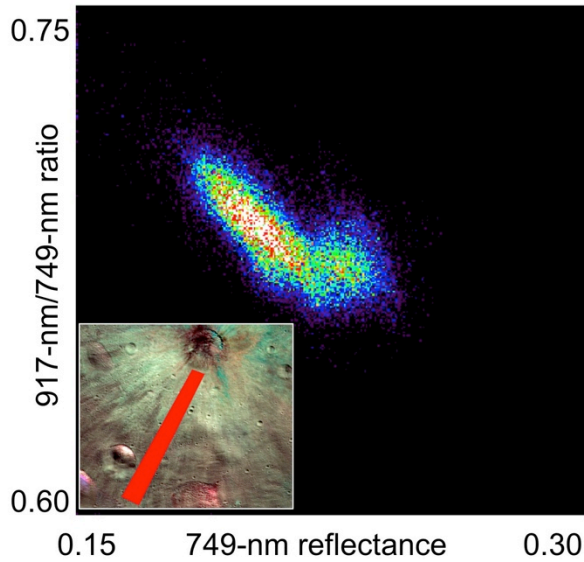


Fig. 1. NIR ratio-reflectance 2D scatterplot for the image ROI (red rectangle) to the SW of Vibidia crater shown in the inset. Vibidia's diameter is 8 km.

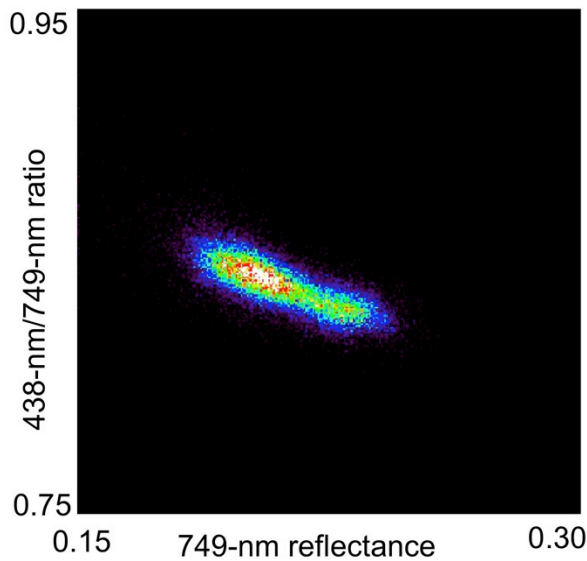


Fig. 2. Vis ratio-reflectance 2D scatterplot for the image ROI to the SW of Vibidia crater shown in Fig. 1.

**References:** [1] C.T. Russell et al. (2012), *Science* 336, 684–686. [2] R. Jaumann et al. (2012), *Science* 336, 687–690. [3] C.M. Pieters et al. (2012) *Nature* 491, 79–82. [4] T.B. McCord et al. (2012), *Nature* 491, 83–86. [5] V. Reddy et al. (2012), *Icarus* 221, 544–559. [6] M.C. De Sanctis et al. (2012), *Ap. J. Lett.* 758, L36. [7] T.H. Prettyman et al. (2012), *Science* 338, 242–246. [8] J. Adams and R. Jones (1970), *Science* 167, 737–739. [9] E. Fischer and C.M. Pieters (1994), *Icarus* 111, 475–488. [10] B. Hapke (2001), *JGR* 106, 10039–10073. [11] S.E. Schröder et al. (2013), *Icarus*

226, 1304–1317. [12] S.E. Schröder et al. (2013), *PSS* 85, 198–213. [13] T. Roatsch et al. (2012), *PSS* 73, 283–286. [14] M.C. De Sanctis et al. (2012), *Science* 336, 697–700. [15] M.C. De Sanctis et al. (2012), *AJL* 758, L36. [16] M.C. De Sanctis et al. (2013), *MPS* 48, 2166–2184. [17] T. Kneissl et al. (2014), *Icarus*, in review. [18] V. Reddy (2012), *Science* 336, 700–704. [19] L. Le Corre et al. (2013), *Icarus* 226, 1568–1594. [20] D.T. Blewett et al. (2011), *LPS* 42, abstr. 1044. [21] K. Stockstill-Cahill et al. (2014), *JGR*, submitted.

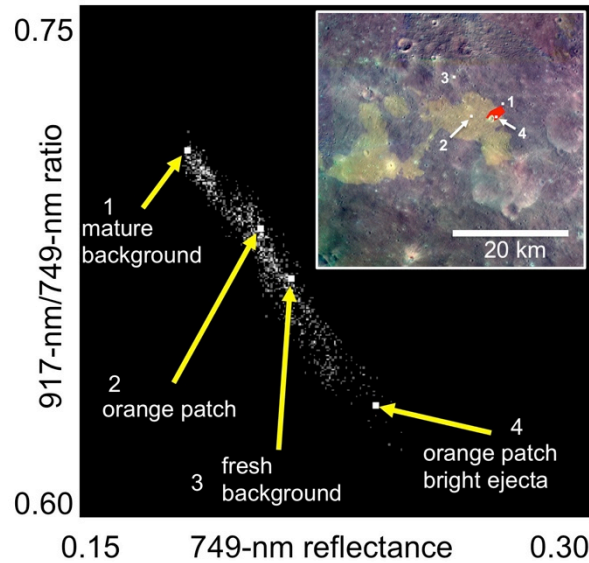


Fig. 3. NIR ratio-reflectance 2D scatterplot for the image ROI (small red polygon) on the patch of unusual material shown in the inset. The locations of individual extracted FC spectra are shown with the arrows.

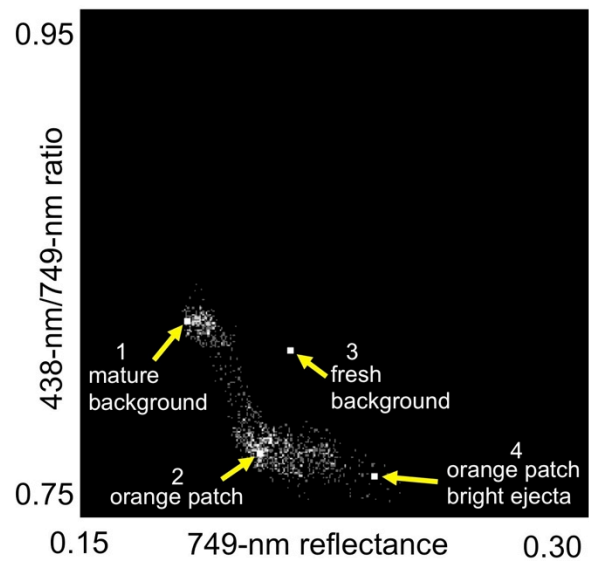


Fig. 4. Vis ratio-reflectance 2D scatterplot for the ROI on the patch of unusual material shown in Fig. 3.